Contribution of Cooking Emissions to the Urban Volatile Organic Compounds in Las Vegas, NV

Matthew M. Coggon.[1*], Chelsea E. Stockwell.[1,2], Lu Xu[1,2,a], Jeff Peischl[1,2], Jessica B. Gilman[1],
Aaron Lamplugh[1,2,b], Henry J. Bowman[3], Kenneth Aikin[1,2], Colin Harkins[1,2], Qindan Zhu[1,2,c],
Rebecca H. Schwantes[1], Jian He[1,2], Meng Li[1,2], Karl Seltzer[4], Brian McDonald[1], Carsten
Warneke[1]

[1] NOAA Chemical Sciences Laboratory (NOAA CSL), Boulder, CO, USA
[2] Cooperative Institute for Research in Environmental Sciences, University of Colorado Boulder,
Boulder, CO, USA
[3] Department of Physics and Astronomy, Carleton College, Northfield, MN, USA
[4] U.S. Environmental Protection Agency, Triangle Park, NC, USA
[a] now at Department of Energy, Environmental and Chemical Engineering, Washington
University in St. Louis, Missouri, USA
[b] now at Institute of Behavioral Science, University of Colorado, Boulder, CO, USA
[c] now at Department of Earth, Atmospheric and Planetary Sciences, Massachusetts Institute of
Technology, Cambridge, MA, USA

*corresponding author: matthew.m.coggon@noaa.gov

Abstract

Cooking is a source volatile organic compounds (VOCs) that degrades air quality. Cooking VOCs
have been investigated in laboratory and indoor studies, but the contribution of cooking to the
spatial and temporal variability of urban VOCs is uncertain. In this study, a proton-transfer-
reaction time-of-flight mass spectrometer (PTR-ToF-MS) is used to identify and quantify cooking
emission in Las Vegas, NV with supplemental data from Los Angeles, CA and Boulder, CO.
Mobile laboratory data show that long-chain aldehydes, such as octanal and nonanal, are
significantly enhanced in restaurant plumes and regionally enhanced in areas of Las Vegas with
high restaurant density. Correlation analyses show that long-chain fatty acids are also associated
with cooking emissions and the relative VOC enhancements observed in regions with dense
restaurant activity are very similar to the distribution of VOCs observed in laboratory cooking
studies. Positive matrix factorization (PMF) is used to quantify cooking emissions from ground
site measurements and compare the magnitude of cooking to other important urban sources, such
as volatile chemical products and fossil fuel emissions. PMF shows that cooking may account for
as much as 20% of the total anthropogenic VOC emissions observed by PTR-ToF-MS. In contrast,
emissions estimated from county-level inventories report that cooking accounts for less than 1%
of urban VOCs. Current emissions inventories do not fully account for the emission rates of long-

40 chain aldehydes reported here and further work is likely needed to improve model representations
41 of important aldehyde sources, such as commercial and residential cooking.
42
43 **1. Introduction**
44
45   Volatile organic compounds (VOCs) degrade air quality and are emitted to urban air from
46 many sources, including fossil fuel combustion (Warneke et al., 2012), the use of volatile chemical
47 products (VCPs, McDonald et al., 2018), industrial processes (Zhang et al., 2004), residential
48 heating and wood burning (e.g., McDonald et al., 2000;Coggon et al., 2016), cooking (Wernis et
49 al., 2022), and urban vegetation (e.g., Churkina et al., 2017). Each source emits a diverse set of
50 molecules that react alongside nitrogen oxides ($NO + NO_2 = NO_x$) to form ozone. Recent field
51 work in major US metropolitan areas has characterized the distribution of urban VOCs to assess
52 the chemical fingerprint of understudied emission sources, such as VCPs (Gkatzelis et al.,
53 2021b;Peng et al., 2022). These studies have shown that these sources emit oxygenated VOCs
54 (oVOCs) which react to form ozone and secondary organic aerosol. Models have been updated to
55 better describe the emissions and chemistry of select oVOCs, including alcohols, siloxanes,
56 glycols, and furanoids (Coggon et al., 2021;Pye et al., 2023;Qin et al., 2021).
57
58   Many oVOCs are emitted to urban air that have not been well-studied or incorporated into
59 air quality models (Karl et al., 2018). For example, McDonald et al. (2018) showed that $C > 5$
60 aldehydes measured in Los Angeles, CA could not be explained by emissions inventories that
61 contain VCPs, fossil fuels, or biogenic sources. Cooking is a source of oVOCs that is rich in
62 aldehydes and fatty acids (Klein et al., 2016a). Cooking VOCs have been extensively characterized
63 in the laboratory (Bastos and Pereira, 2010;Klein et al., 2016a;Klein et al., 2016b;Schauer et al.,
64 1999;Zhao and Zhao, 2018) and it has been shown that cooking is a key activity controlling the
65 budget of VOCs measured in indoor air (Arata et al., 2021;Klein et al., 2019;Klein et al., 2016a).
66 Numerous studies have shown that cooking is a ubiquitous and important component of organic
67 aerosol in urban areas (Hayes et al., 2013;Robinson et al., 2006;Robinson et al., 2018;Shah et al.,
68 2018;Slowik et al., 2010;Zhang et al., 2019) yet only a few studies have been conducted to
69 characterize cooking VOCs in ambient datasets (e.g., Peng et al., 2022;Wernis et al., 2022).
70
71   Cooking emissions result from the combustion and high temperature decomposition of
72 food and oils (Bastos and Pereira, 2010;Umano and Shibamoto, 1987). During heating, fatty acids
73 undergo thermal oxidation to produce emissions of aldehydes, ketones, alcohols, acids, and other
74 products of depolymerization (Bastos and Pereira, 2010;Schauer et al., 1999). The use of spices
75 emits monoterpenes and their derivatives (Klein et al., 2016a). Studies that have speciated VOCs
76 from a variety of Western cooking styles (e.g., charbroiling, grilling, frying) and ingredients (e.g.,
77 oils, meats, and vegetables) show that aliphatic C_1-C_{11} aldehydes account for a large fraction of
78 VOCs measured by gas-chromatography and mass spectrometry (e.g., Bastos and Pereira,
79 2010;Klein et al., 2016b;Peng et al., 2017;Schauer et al., 1999). For example, Klein et al. (2016b)

80   reported that aldehydes represent > 60% of the VOC mass emitted from frying or charbroiling
81   meats and vegetables.
82
83   Ambient observations have shown that long-chain aldehydes are present in urban air at
84   significant mixing ratios (e.g., nonanal ~ 100 – 200 ppt, Bowman et al., 2003;Wernis et al., 2022).
85   Recent studies have used hexanal and nonanal as markers for cooking emissions in in Atlanta, GA
86   and Livermore, CA (Peng et al., 2022;Wernis et al., 2022). These species correlated with morning
87   and evening meal preparation, and it was suspected that restaurant emissions were a driving factor
88   for the observed temporal variability in Livermore (Wernis et al., 2022). In addition to cooking,
89   certain long-chain aldehydes are known to be emitted from diesel exhaust (e.g., hexanal, Gentner
90   et al., 2013), and some are produced from the emission and ozonolysis of oils and fatty acids
91   present in human skin, at the surface of ocean waters, or from other surfaces that contain
92   unsaturated lipids (Kruza et al., 2017;Liu et al., 2021;Wang et al., 2022;Kilgour et al., 2021).
93
94   The high abundance of aliphatic aldehydes from cooking suggests that they may be useful
95   markers to constrain cooking VOC emissions in urban areas. The utility of aldehydes as cooking
96   markers relies on the characterization of their sources in the atmosphere as well as careful
97   characterization of measurement techniques used to detect these species. Short-chain aldehydes
98   (C< 5) are unlikely to serve as useful markers because they are produced in the atmosphere from
99   the OH oxidation of primary organic molecules and are also directly emitted from fossil fuel
100 emissions and biomass burning (Gentner et al., 2013;Koss et al., 2018;de Gouw et al., 2018). Long-
101 chain aliphatic aldehydes (C > 6) have the potential to be useful markers for cooking in urban
102 areas, but their primary sources, spatial distributions, and abundances in the atmosphere remain
103 uncertain. Some long-chain aldehydes may be emitted from mobile sources (e.g.,Gentner et al.,
104 2013) while others may be emitted from surface ozone chemistry (e.g., Liu et al., 2021). No field
105 measurements have reported the spatial distribution of long-chain aldehydes to determine likely
106 sources in urban air.
107
108   This study evaluates the contribution of commercial and residential cooking emissions to
109 urban VOCs using mobile laboratory and ground site observations in Las Vegas, NV with
110 supplemental observations made Los Angeles, CA and Boulder, CO. Mobile laboratory
111 measurements show that long-chain aliphatic aldehydes are significantly enhanced downwind of
112 restaurants and exhibit spatial distributions in urban regions of Las Vegas that closely matches
113 restaurant density. Furthermore, these measurements show that the distribution of VOCs that
114 correlate with long-chain aldehydes strongly resembles the distribution observed in restaurant
115 plumes. We conduct a source apportionment analysis to determine the extent to which cooking
116 emissions impact urban VOCs relative to other important anthropogenic sources, such as motor
117 vehicles and VCPs, and compare these observations to commonly used emissions inventories.
118
119

2. Methods

2.1. Field Campaign Description

Air quality measurements were performed during the 2021 Southwest Urban NO_x and VOC Experiment (SUNVEx) and Re-Evaluating the Chemistry of Air Pollutants in California (RECAP-CA) studies. Trace gases were measured from the NOAA mobile laboratory and at ground sites located at the Jerome Mack Air Quality Station in Las Vegas, NV and the California Institute of Technology campus in Pasadena, CA. In Las Vegas, seven mobile laboratory drives were conducted between 27 June and 31 July, 2021 with a focus on sampling densely populated regions. Ground sampling was primarily conducted from 30 June– 27 July, 2021.

Figure 1 is a map of the Las Vegas valley that shows the locations of residential, commercial, and entertainment districts. The blue dots show the locations of restaurants that are cataloged in health inspection reports maintained by the Southern Nevada Health District (SNHD, 2022). The wind rose is centered at the Jerome Mack Air Quality Station and shows the prevailing wind directions and speeds observed at the ground site. The mobile laboratory sampled across the region (e.g., Figure 3), but focused drives was conducted along the Las Vegas Strip (the purple shaded region shown in Fig. 1). The Las Vegas Strip is an entertainment district with a high density of casinos, hotels, bars, and restaurants that emit VCP, fossil fuel, and cooking VOCs. The Jerome Mack ground site is located ~8km northeast of the Las Vegas Strip in a residential area with restaurants and small commercial businesses located along major streets. The prevailing wind patterns show that ground measurements were routinely impacted by air transported from the Las Vegas Strip along with regions to the north with higher commercial activity.

Ground measurements during RECAP-CA were performed at the California Institute of Technology in Pasadena, CA from 1 August – 5 September, 2021. These measurements serve as a comparison to the observations in Las Vegas. VOCs and other trace gases were sampled from the top of a 10 m tower. The location of the ground site was located within 0.5km from the ground site used during the 2010 CalNex campaign (Ryerson et al., 2013). The Pasadena ground site has been previously characterized and is a downwind receptor site for air impacted by emissions from downtown Los Angeles, CA (e.g., de Gouw et al., 2018).

Supplemental mobile laboratory measurements were performed in Los Angeles, CA and Boulder, CO to sample VOCs downwind of individual restaurants. These measurements serve as comparisons against the restaurant emissions observed in the Las Vegas region.
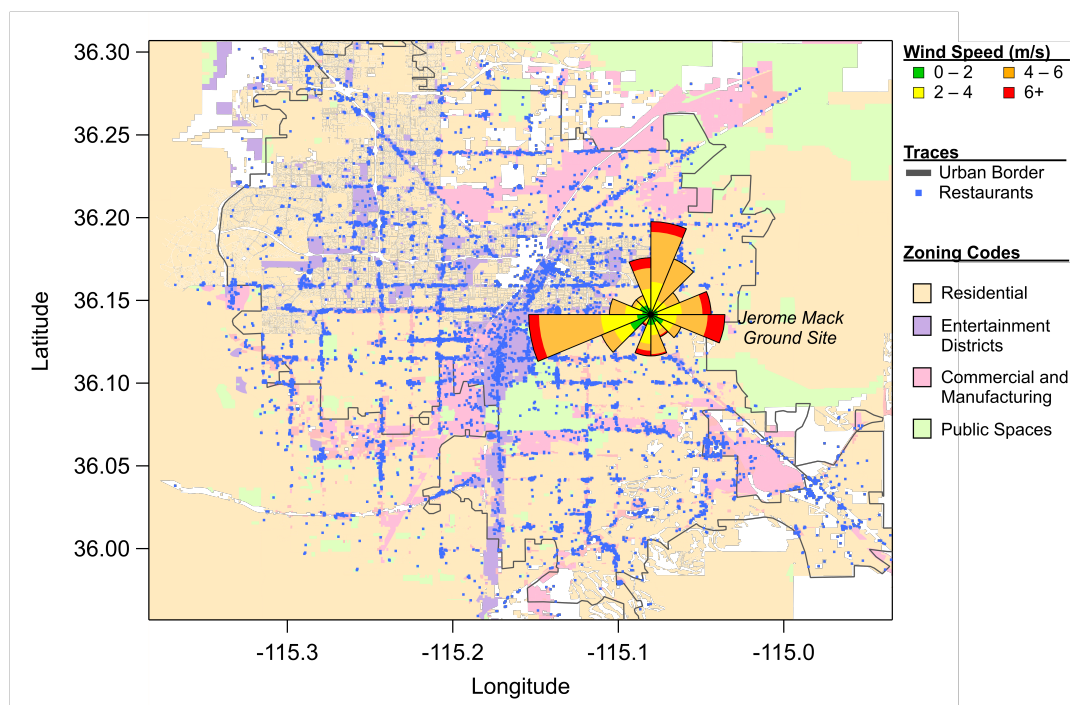
Figure 1: Zoning map of the Las Vegas region showing areas permitted for residential buildings, entertainment districts, commercial and manufacturing use, and public spaces. Data are available from the Clark County GIS Management Office (https://clarkcountygis-ccgismo.hub.arcgis.com, accessed September 2023) The blue dots show the locations of restaurants in the Las Vegas valley that are cataloged in health inspection reports maintained by the Southern Nevada Health District (SNHD, 2022). The wind rose shows the prevailing wind directions and speed observed at the Jerome Mack ground site. The wind rose is centered on the map at the location of Jerome Mack.

2.2. Instrument Description

PTR-ToF-MS

VOC mixing ratios were measured using a Vocus proton-transfer-reaction time-of-flight mass spectrometer (PTR-ToF-MS) (Yuan et al., 2016;Krechmer et al., 2018). The PTR-ToF-MS measures a large range of aromatics, alkenes, nitrogen-containing species, and oxygenated VOCs. A full description of the instrument during SUNVEx is provided by Coggon et al. (2023). Briefly, the PTR-ToF-MS sampled air a ~2 L min^{-1} through a short (< 1m) inlet while in the mobile laboratory. At the ground sites, the instrument sampled at ~20 L min^{-1} from a 10 m tower. The Vocus drift tube was operated at 110°C with an electrical field (E) to number density (N) ratio (E/N) of 140 Td. Instrument backgrounds were determined every 2 h for ground site experiments and every ~15-30 minutes during drives by passing air through a platinum catalyst heated to 350°C.

179   Data were processed following the recommendations of Stark et al. (2015) using the Tofware
180   package in Igor Pro (WaveMetrics). The PTR-ToF-MS was calibrated using gravimetrically-
181   prepared gas standards for typical VOCs such as acetone, methyl ethyl ketone, toluene, and C8-
182   aromatics. Many compounds unavailable in gas standards were quantified by liquid calibration
183   methods as described by Coggon et al. (2018). This included D5-siloxane,
184   parachlorobenzotriflouride, octanal and nonanal. All other compounds were quantified using
185   estimated proton-transfer-reaction rate constants as described by Sekimoto et al. (2017). Further
186   corrections were applied to masses assigned to long-chain aldehydes based on observed mass-
187   dependent changes in fragmentation patterns described in the Supplemental Information and
188   shown in Fig. S2.

189

190   PTR-ToF-MS only resolves VOC molecular formula. To identify structural isomers, a
191   custom-built gas-chromatography (GC) instrument was used to collect and pre-separate VOCs
192   prior to detection by PTR-ToF-MS. A full description of the system is provided by Stockwell et
193   al. (2021) and its operation during SUNVEx is described by Coggon et al. (2023). Briefly, the GC
194   consists of a DB-624 column (Agilent Technologies, 30 m, 0.25 mm ID, 1.4 µm film thickness)
195   and oven identical to the system described by Lerner et al. (2017). VOCs were condensed onto a
196   liquid nitrogen cryotrap, flash vaporized, then passed through the column using nitrogen as a
197   carrier gas. The column was linearly heated during separation from 40-150°C. The effluent from
198   the column was directly injected in the PTR-ToF-MS inlet. At the Jerome Mack ground site, GC
199   samples were collected every 2 hours and immediately analyzed by PTR-ToF-MS. GC samples
200   were also collected during a nighttime mobile laboratory drive on July 31, 2021. These samples
201   were used to help interpret PTR-ToF-MS measurements along the Las Vegas Strip.

202

203   A key goal of this study is to characterize the spatial and temporal pattern of long-chain
204   aldehydes. Aldehydes and ketone isomers are quantified by PTR-ToF-MS using measurements of
205   the proton-transfer product ions (= VOC mass + H^+). Aliphatic aldehydes also undergo
206   dehydration (= VOC mass + H^+ – H_2O) and fragmentation reactions, which effectively lowers the
207   instrument sensitivity to the proton-transfer product. Consequently, it can be challenging to
208   unambiguously assign carbonyl ions to specific isomers. In the Supplemental Information, GC-
209   PTR-ToF-MS and mobile laboratory PTR-ToF-MS measurements show that C_8 and C_9 carbonyls
210   measured in urban areas are predominantly associated with octanal (detected at m/z 129,
211   $C_8H_{16}OH^+$) and nonanal (detected at m/z 143, $C_9H_{18}OH^+$). These ions have no detectable
212   interferences from ketone isomers in GC-PTR-ToF-MS spectra (Fig. S1) and the ratio of these
213   ions with carbonyl dehydration products most closely matches the fragmentation patterns of
214   aldehydes (Fig. S3). Smaller carbonyls have significant interferences from ketone isomers, which
215   complicates their use as markers for aldehyde emissions. Here, we focus on the spatial and
216   temporal trends of octanal and nonanal and use these markers to determine the fingerprint of
217   cooking VOC emissions.

218

LGR Carbon Monoxide

Carbon monoxide was measured at the Caltech ground site from a 10 m stainless steel tube (3.2 mm OD, 1.6 mm ID) using off-axis integrated cavity output spectroscopy (ABB Inc./Los Gatos Research model F-N$_2$O/CO-23r) (Roberts et al., 2022). Data were measured at 1-Hz and reported as 1-minute averages. Instrument precision was estimated to be ±0.2 ppb (1-σ), and the 1-σ uncertainty was estimated to be ±1% based on calibrations in the laboratory before and after the SUNVEx/RECAP-CA project.

2.3. Positive Matrix Factorization

Positive matrix factorization (PMF) is used to analyze the PTR-ToF-MS data and apportion VOCs to cooking and other urban sources in Las Vegas. PMF was conducted using the Source Finder (SoFi) software package in Igor Pro (Canonaco et al., 2013). Two periods are analyzed when PTR-ToF-MS measurements were available: 30 June–9 July and 19–27 July. In this analysis, we constrain PMF with a mobile source profile derived from mobile measurements following the recommendations of Gkatzelis et al. (2021b). We present a solution of factors representing mobile sources, VCPs, cooking, and regional chemical oxidation. A full description of the PMF analysis is provided in the Supplemental Information.

3. Results

3.1. Long-chain aldehydes downwind of restaurants

Previous studies have shown that cooking organic aerosols (COA) from dense restaurant clusters exhibit plume-like behavior that can impact local air quality at spatial scales of 0.5–1 km (Robinson et al., 2018;Shah et al., 2018). For example, Robinson et al. (2018) showed that organic aerosol was enhanced by as much as 100–200 µg m^{-3} within 1 km of restaurants and resulted in average local organic aerosol enhancements of 3.2 µg m^{-3}. Consequently, it is expected that VOCs would also be significantly enhanced in close proximity of restaurants.

Figure 2 shows mobile laboratory measurements of nonanal and octanal mixing ratios downwind of two fast food restaurants in Los Angeles, CA and Boulder, CO. Mixing ratios of markers typically representative of personal care products (D5-siloxane) and motor vehicle emissions (benzene) are also shown to highlight the presence of other sources in the region. The restaurant in Los Angeles primarily serves hot dogs, while the restaurant in Boulder serves hamburgers and fried foods. The highlighted boxes show periods where the mobile laboratory was parked to sample restaurant emissions. All other data reflect sampling periods when the mobile laboratory was driven through densely populated areas of Los Angeles and Boulder. In both cases, the mobile laboratory was parked within 50m of the restaurant exhausts.

259

260   Aldehyde mixing ratios downwind of both restaurants exceeded 1 ppb. Generally, these
261 mixing ratios were elevated relative to the surrounding densely populated regions. Octanal and
262 nonanal mixing ratios were not significantly enhanced in tailpipe emissions, which is consistent
263 with previous studies showing that on-road emission factors of these from US vehicles are low
264 (Gentner et al., 2013). Octanal and nonanal were not strongly correlated with mixing ratios of D5-
265 siloxane, though there were periods when long-chain aldehyde and D5-siloxane enhancements
266 were coincident. This may result from the co-location of food and people or a possible human
267 emission source. Octanal and nonanal are known to be produced from skin ozonolysis (Liu et al.,
268 2021;Wang et al., 2022) and carbonyls are potential ingredients in fragranced consumer products,
269 though emissions inventories and measurements of fragrance formulations do not indicate that
270 octanal and nonanal are significant ingredients of VCPs (Hurley et al., 2021;McDonald et al.,
271 2018;Yeoman et al., 2020).

272
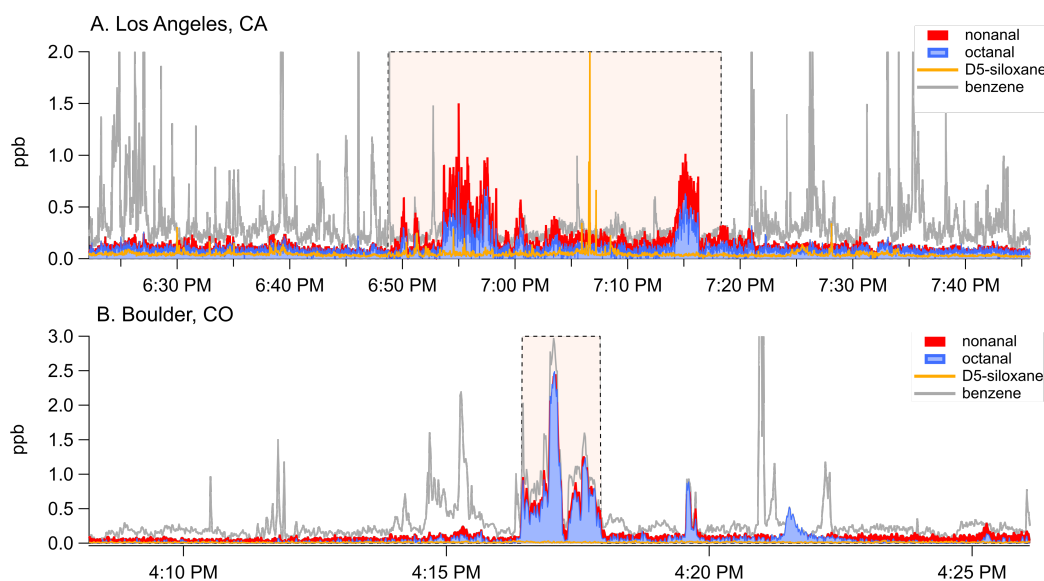
273
274 **Figure 2:** Mobile laboratory measurements of octanal, nonanal, D5-siloxane, and benzene in (A) Los
275 Angeles, CA and (B) Boulder, CO. The shaded regions show periods when the mobile laboratory was
276 parked downwind of a restaurant that primarily serves hot dogs (Los Angeles) and a restaurant that primarily
277 serves hamburgers (Boulder). All other data were collected while the mobile laboratory sampled air in
278 populated areas.

279

280   Figure 2 shows that restaurants are a strong source of aliphatic aldehydes, such as octanal and
281 nonanal. Based on these enhancements, it is likely that VOCs emitted from cooking are
282 significantly enhanced in regions with dense restaurant activity. These inferences are consistent
283 with previous mobile laboratory observations of primary organic aerosols. For example, Robinson

284   et al. (2018) found that organic aerosol in commercial districts of Pittsburgh, PA with significant
285   restaurant density was nearly twice as concentrated as organic aerosol in areas with highways and
286   significant traffic. Similar results were observed by Shah et al. (2018) in Oakland, CA where COA
287   constituted ~ 50% of the primary organic aerosol and was observed to be enhanced in downtown
288   regions where restaurant density was highest. Both studies demonstrate that air quality in urban
289   areas is significantly impacted by restaurant density.
290
291   Las Vegas is a sprawling city where most emission sources are concentrated along the Las
292   Vegas Strip (Figure 1). Figure 3 shows the spatial distribution of octanal and nonanal from all of
293   the mobile laboratory drives, along with a map of restaurant density calculated using the restaurant
294   location data shown in Figure 1. Each pixel is determined by summing the number of restaurants
295   over a 0.5 x 0.5 km grid. Figure 3 shows that octanal and nonanal are well-correlated ($R^2 = 0.82$)
296   and predominantly enhanced in the Las Vegas Strip area where anthropogenic emissions are the
297   highest. Figure 3A shows that this region has a high restaurant density compared to other regions
298   of the Las Vegas Valley. We note that brief (~1s), isolated enhancements in PTR-ToF-MS
299   measurements of octanal are observed outside of the Las Vegas Strip. These enhancements also
300   have corresponding increases in nonanal, though the ratios of these species are different than what
301   is observed along the Las Vegas Strip.
302
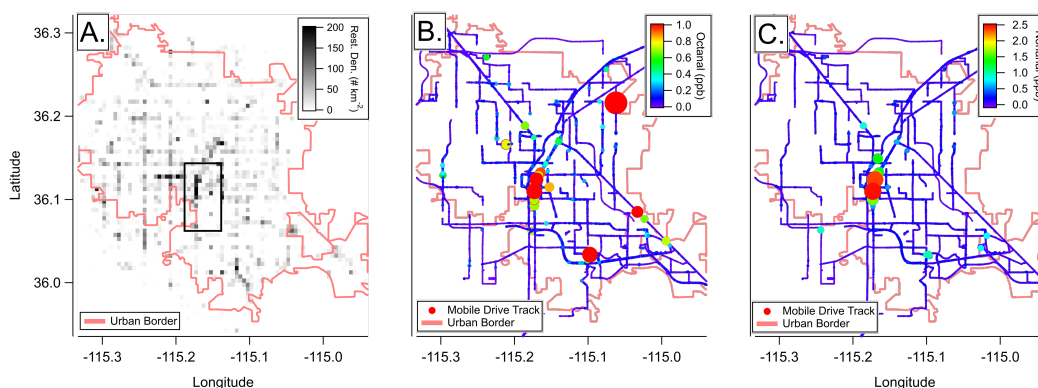
305   **Figure 3:** (A) Restaurant density in Clark County, NV. Restaurant density is determined using the
306   restaurant locations shown in Fig. 1 and is calculated by summing the number of restaurants located within
307   a 0.5 x 0.5 km grid. The rectangle shows the approximate region of the Las Vegas Strip. Panels (B) and (C)
308   show the mobile laboratory path colored by octanal and nonanal mixing ratios, respectively. Markers are
309   sized by the corresponding mixing ratios shown in the color scales.
310

311   Figure 4 further evaluates the spatial distribution of long-chain aldehydes by comparing
312   nonanal mixing ratios against the restaurant density in the proximity of the mobile laboratory.
313   Here, restaurant density is extracted from Fig. 3A by selecting the grid cells that are coincident
314   with the mobile laboratory position while sampling in the vicinity of the Las Vegas Strip (indicated

315   by the black box shown in Fig. 3A). The three drives shown correspond to mid-day (12:00 – 7:00
316   PM local time), evening (8:00 – 11:00 PM), and late-night (9:30 PM – 1:00 AM) sampling. The
317   drives show that nonanal is generally enhanced in regions with higher restaurant density. Nonanal
318   mixing ratios are highest during evening drives when activities from the entertainment industry in
319   the Las Vegas Strip area, including dining, are likely most frequent (panels B and C).
320   Enhancements in nonanal are also observed during a mid-day drive (panel A), though mixing ratios
321   are generally lower due to a higher boundary layer and potentially lower emissions in the Las
322   Vegas Strip area during the day. Octanal exhibits a similar relationship with restaurant density.
323   These results are consistent with the observed enhancements in organic aerosol seen previously
324   observed in dense restaurant regions (Robinson et al., 2018;Shah et al., 2018).
325
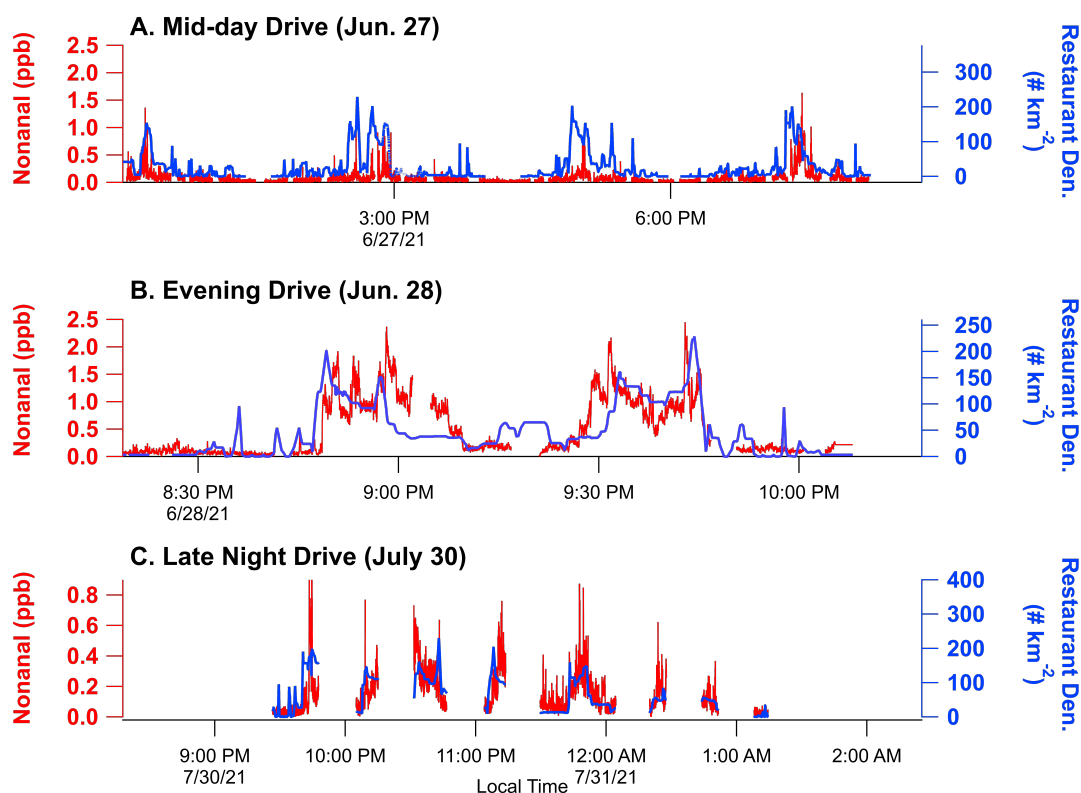
Figure 4: Nonanal mixing ratios and corresponding restaurant density in areas sampled by the mobile
laboratory. Restaurant density is determined by averaging restaurant data in Figure 3A on a 0.5 km x 0.5
km grid, then extracting data along the mobile laboratory drive track.

Figure S12 shows that the octanal and nonanal observed along the Las Vegas Strip are also
measured at the Jerome Mack ground site. The two species are well-correlated ($R^2 > 0.86$) and
most abundant at night, likely due to a combination of meteorology (i.e., shallow nocturnal

335   boundary layer) and higher emissions in the evening (e.g., Fig. 4). Figure S12 also shows octanal
336   and nonanal mixing ratios observed at the Caltech ground site in Pasadena, CA. These
337   measurements exhibit similar temporal behavior and demonstrate that long-chain aldehyde are
338   ubiquitous in many urban regions. We note that nonanal ratios reported here are similar to those
339   observed from previous studies (~ 100 – 200 ppt, Bowman et al., 2003;Wernis et al., 2022).

340

341   **3.2. Species co-emitted with octanal and nonanal in the Las Vegas Strip**

342

343   Octanal and nonanal represent a significant fraction of cooking VOCs measured in laboratory
344   studies (>5%) but are just two of many VOCs emitted from cooking activities (Klein et al., 2016b).
345   To assess the potential fingerprint of VOCs in regions impacted by commercial cooking, we
346   evaluate the VOC mass spectra from the Las Vegas Strip and identify cooking VOCs by correlating
347   PTR-ToF-MS ions to observations of nonanal. Species are only included in this analysis if the
348   detected ion likely represents a proton-transfer product (i.e., fragments are excluded) and correlates
349   with nonanal with $R^2 > 0.8$. This high correlation coefficient is used to identify potential co-emitted
350   species, while excluding VOCs emitted from sources that are co-located with restaurants in the
351   Las Vegas Strip, such as mobile sources and VCPs. For example, D5-siloxane correlates with
352   nonanal with an R^2 of 0.78. Personal care product emissions are significant along the Las Vegas
353   Strip (D5-siloxane mixing ratios > 1 ppb on June 28, 2021), but octanal and nonanal have not been
354   reported as major components of fragranced personal care products (e.g., McDonald et al.,
355   2018;Steinemann, 2015;Steinemann et al., 2011;Yeoman et al., 2020;Hurley et al., 2021). A high
356   correlation is expected because food and people are co-located; however, in this analysis D5-
357   siloxane and compounds with $R^2 < 0.8$ are excluded.

358

359   Figure 5 shows the correlation spectrum of the VOCs to nonanal. The correlation coefficient
360   and the ratio of VOCs to nonanal are plotted versus the detected mass. The compounds that
361   correlate with nonanal have chemical formula of either C_xH_yO or $C_xH_yO_2$ with carbon numbers
362   ranging between $C_2 – C_{11}$. Compounds with formula C_xH_yO are likely aliphatic aldehydes with
363   varying degrees of saturation and some key species are highlighted for each carbon grouping
364   (Figure 6A). Species with the highest correlation to nonanal include octenal ($R^2 = 0.94$), decenal
365   ($R^2 = 0.93$), butenal/crotonaldehyde ($R^2 = 0.93$), and acrolein ($R^2 = 0.92$). While individual $C_3 –$
366   C_5 species are the largest contributors to the total signal, the sum of long-chain aldehydes ($C_6 –$
367   C_{11}) are >50% of the total spectrum.

368

369   Compounds with formula $C_xH_yO_2$ likely correspond to fatty acids (Figure 5B). Gaseous acids
370   are released from the high temperature decomposition of long-chain acids present in meat and
371   previous studies have measured significant emissions of heptanoic, octanoic, nonanoic, and
372   decanoic acid (Schauer et al., 1999;Klein et al., 2016b). The acids in Figure 5B are some of the
373   most abundant acids observed along the Las Vegas Strip. The strong correlation of nonanal to fatty
374   acids further supports that cooking emissions are an important emitter of long-chain aldehydes in
375   this region.

376
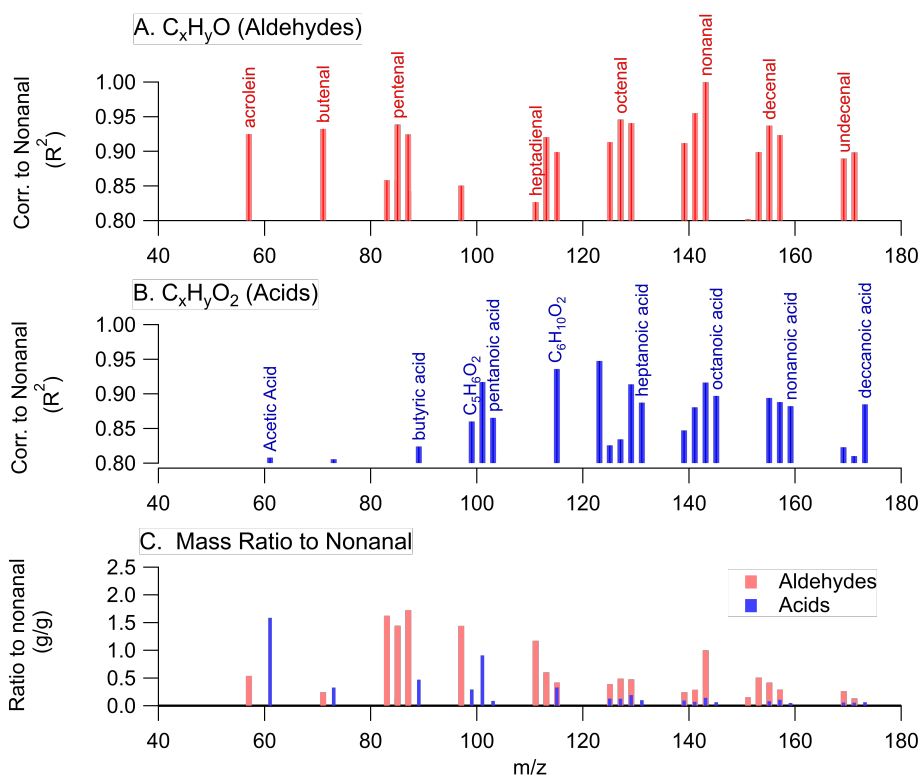
377
Figure 5: VOC correlation to nonanal in downtown Las Vegas during nighttime mobile sampling for (A)
C_xH_yO species (assigned as aldehydes) and (B) $C_xH_yO_2$ species (assigned as acids). (C) VOC / nonanal
ratios for species that correlate with nonanal with $R^2 > 0.8$.

Figure 6 compares the spectra measured along the Las Vegas Strip to the spectra derived from
the individual restaurants sampled in Boulder, CO and Los Angeles, CA (Figure 2). The VOC
ratios observed in the restaurant plumes are strikingly similar to the ratios observed in downtown
Las Vegas. The Las Vegas samples most resemble those observed downwind of the hot dog
restaurant in Los Angeles. The two spectra are well correlated ($R^2 = 0.82$) which further supports
that the aldehydes and acids measured along the Las Vegas Strip were associated with restaurant
emissions. The spectra are also comparable to available PTR-ToF-MS spectra of meat cooking
emissions reported by Klein et al. (2016b). These laboratory measurements show that heptadienal,
octanal, nonanal, decadienal, and undecanal are key $C_7 – C_{11}$ aldehydes emitted when cooking
meats with vegetable oils. The same aldehydes are observed in the Las Vegas Strip area.
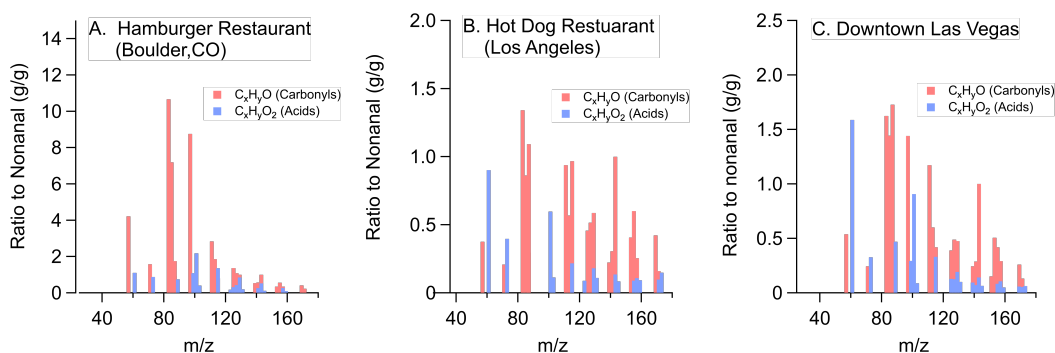
Figure 6. Comparison of (A) restaurant emissions from a hamburger restaurant in Boulder, CO, (B) restaurant emissions from a hot dog restaurant in Los Angeles, and (C) cooking emissions from measurements along the Las Vegas Strip.

Klein et al. (2016b) speciated laboratory cooking emissions and distinguished emissions of higher carbon aldehydes (C ≥ 7) and acids from lower carbon species. These groupings are also distinct in the laboratory VOC distributions reported by Schauer et al. (1999) and are suspected to be signatures of cooking emissions in Las Vegas (e.g., Fig. 5). Figure 7 compares the distribution of C ≥ 7 oxygenates observed in this study (top row) with the distributions reported by laboratory studies (bottom row). Schauer et al. (1999) observed that ~10% of the C ≥ 7 mass emitted from beef charbroiling was attributed to acids, while 90% was attributable to carbonyls largely composed of aldehydes. Klein et al. (2016b) observed a similar profile averaged across a range of experiments using meats and vegetable oils. In the Las Vegas Strip area, acids represented ~16% of mass associated with C ≥ 7 compounds, while the remainder is associated with carbonyls dominated by aldehydes. Carbonyls are the dominant C ≥ 7 emissions from both restaurants sampled by the mobile laboratory. The similarity in the distributions between laboratory and field observations further suggest that long-chain aldehydes are useful markers for constraining cooking emissions in urban air.
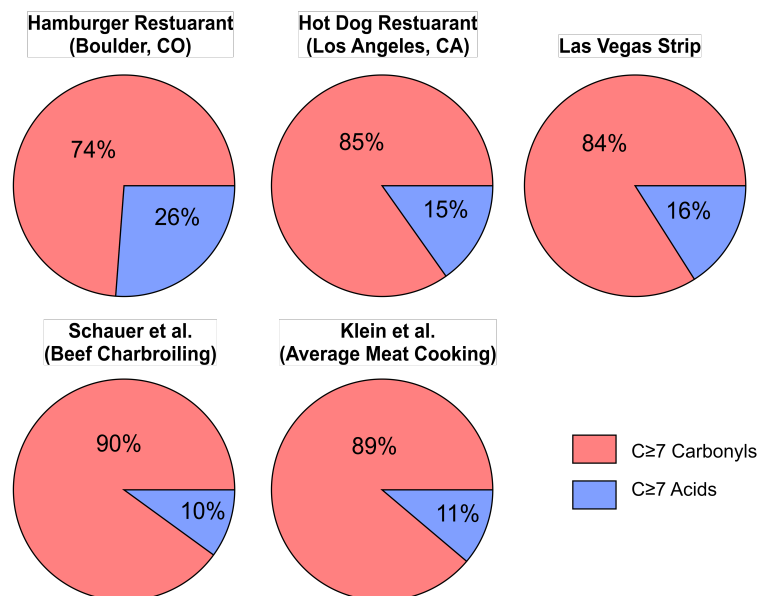
Figure 7: Comparison of the C ≥ 7 oxygenates measured as part of this study (top row) with those observed from laboratory experiments reported by Schauer et al. (1999) and Klein et al. (2016b) (bottom row). The distribution from Schauer et al. (1999) reflects emissions from beef charbroiling, while the distribution from Klein et al. (2016b) is derived as the average distribution from the frying of pork, chicken, beef, and fish in a range of vegetable oils.

4. Source apportionment from Las Vegas measurements

The analysis described in Section 3.2 provides a perspective of the key VOCs emitted from commercial cooking. Other VOCs are also likely associated with cooking but are not resolved by a simple correlation analysis due to the presence of other important sources along the Las Vegas Strip, such as ethanol from VCPs or monoterpenes from fragranced consumer products. Moreover, emissions from residential cooking may also contribute to regional VOC mixing ratios. Here, we discuss the PMF results to determine the emissions profile and the contribution of cooking to total VOC emissions observed at the Jerome Mack ground site.

Figures 8 and 9 show the PMF solution for the data collected at the Jerome Mack ground site. Figure 8 shows the time series and factor profiles, while Fig. 9 shows the average diurnal profiles. We present a 5-factor solution where VOCs are apportioned to (1) a mobile source factor, (2) a VCP-dominated factor, (3) a cooking-dominated factor, (4) a regional background plus secondary oxidation processes, and (5) a local solvent source. A full description of the PMF results is provided in the Supplemental Information.

439   The mobile source factor is largely composed of ethanol and C_6-C_{10} aromatics (Fig. S4). The
440   VCP-dominated factor is primarily composed of ethanol (EOH), but also contains D5-siloxane,
441   monoterpenes, and acetone, which are common ingredients in consumer products. Both factors
442   resemble the solution presented by Gkatzelis et al. (2021b) for New York City. The VCP-
443   dominated factor derived here has two key differences from the factor derived by Gkatzelis et al.
444   (2021b). First, the VCP-dominated factor from New York City contained a series of other VCP
445   markers, including PCBTF and D4-siloxane. These molecules are largely associated with
446   construction activity and are expected to be emitted from the application of industrial coatings and
447   adhesives (Gkatzelis et al., 2021a;Stockwell et al., 2021). At the Jerome Mack ground site, PCBTF
448   variability was largely attributed to the local solvent factor (Fig. 8), which appeared to come from
449   a point source located near the ground site. Second, the VCP-dominated factor reported by
450   Gkatzelis et al. (2021b) also contained methyl ethyl ketone, which is a prominent solvent in
451   consumer and industrial VCPs. Methyl ethyl ketone was excluded from this analysis due to a water
452   cluster interference produced within the Vocus drift tube.
453
454   The oxidation factor is largely composed of multiple oxygenated carbon-containing masses,
455   which agrees with secondary factors resolved by PMF in other cities (Gkatzelis et al., 2021b;Peng
456   et al., 2022). At the Jerome Mack site, this factor also contained VOCs that are emitted during
457   daytime hours from biogenic sources (e.g., isoprene, monoterpenes) due to emissions from urban
458   vegetation. In general, isoprene and monoterpenes had relatively low mixing ratios over the
459   analyzed sampling period (< 150 ppt). For comparison, measurements in Los Angeles during
460   RECAP-CA show that average isoprene mixing ratios exceeded 2 ppb (Coggon et al., 2023). This
461   difference highlights that urban vegetation emissions in Las Vegas are significantly lower than
462   other cities.
463
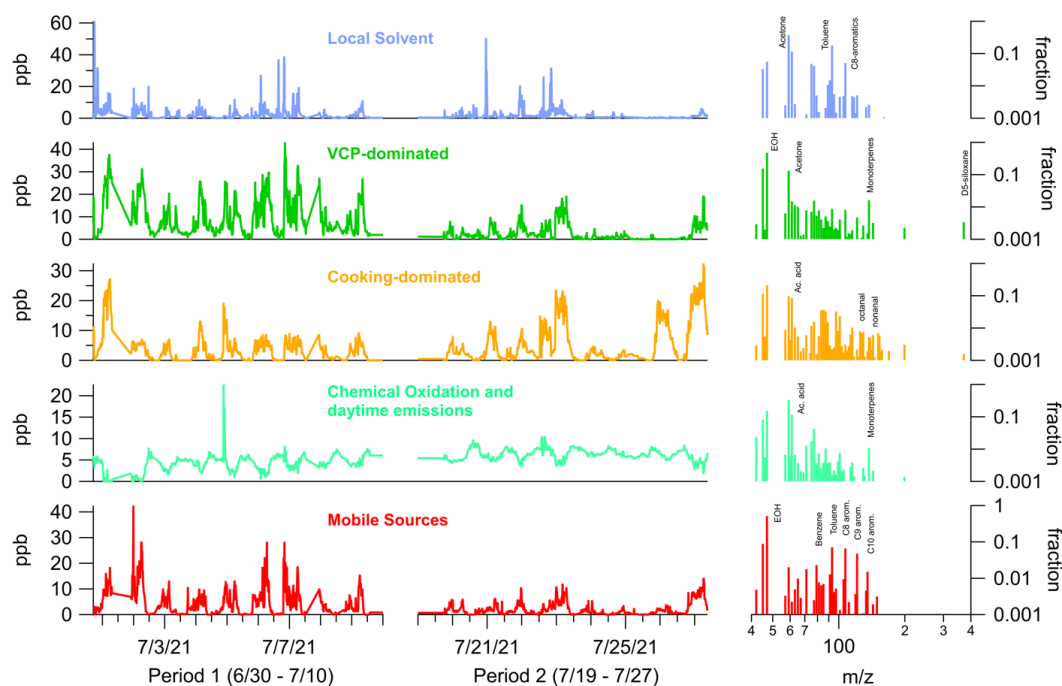
Figure 8: 5-factor PMF solution for the ground site data at Jerome Mack. Shown are the factor time profiles for the two time periods considered for this analysis (Period 1, 30 June–10 July and Period 2, 19–27 July) along with the resolved factor profiles.

PMF of the Jerome Mack data resolves a factor that is enriched in aldehydes, which we interpret as the cooking-dominated factor. This factor includes contributions from octanal, nonanal, acetic acid, acrolein, and higher carbon aldehydes and acids, which is consistent with the cooking emissions observed along the Las Vegas Strip and downwind of restaurants. Figure S10 compares the PMF profile to the VOC/nonanal profiles resolved by the mobile laboratory and shows that the two profiles agree for overlapping species. This agreement supports the PMF resolution of mass associated with important cooking VOCs. The PMF factor also includes ethanol, monoterpenes, and acetone/propanal, which were not resolved by the mobile laboratory analysis. Cooking emits significant amounts of ethanol and monoterpenes to indoor air (Arata et al., 2021;Klein et al., 2016a), and is a dominant source of total VOC emissions in residential indoor air (Arata et al., 2021;Klein et al., 2019). These species represent ~22% of the cooking-dominated factor.

Figure 9 shows daily mass concentrations for each factor. Gkatzelis et al. (2021b) compared the speciation profiles of the VCP-dominated and mobile source profiles to those represented in emissions inventories and found that ~53% of the mass associated with mobile source emissions and ~50% of the mass associated with VCPs results from emissions that cannot be resolved by

16

486   PTR-ToF-MS (e.g., alkanes and small alkenes). The mobile source and VCP-dominated factors
487   shown in Figures 9 and 10 have been adjusted to account for this unresolved mass. No adjustments
488   are applied to the cooking-dominated, solvent, or oxidation factor as it is assumed that PTR-ToF-
489   MS measures the key VOCs from these sources. This may not account for mass that has been
490   previously reported from cooking emissions, such as alkanes or alkenes (Schauer et al., 1999).
491
492   For the mobile source, VCP-dominated, and cooking-dominated factors, mass concentrations
493   are highest at night when the nocturnal boundary layer is shallow. In the daytime, the boundary
494   layer rapidly rises to as high as 4 km (Langford et al., 2022), and VOC concentrations decrease in
495   response. In contrast, the chemical oxidation + daytime emissions factor increases during daytime
496   hours, further supporting that this factor is largely driven by secondary processes.
497
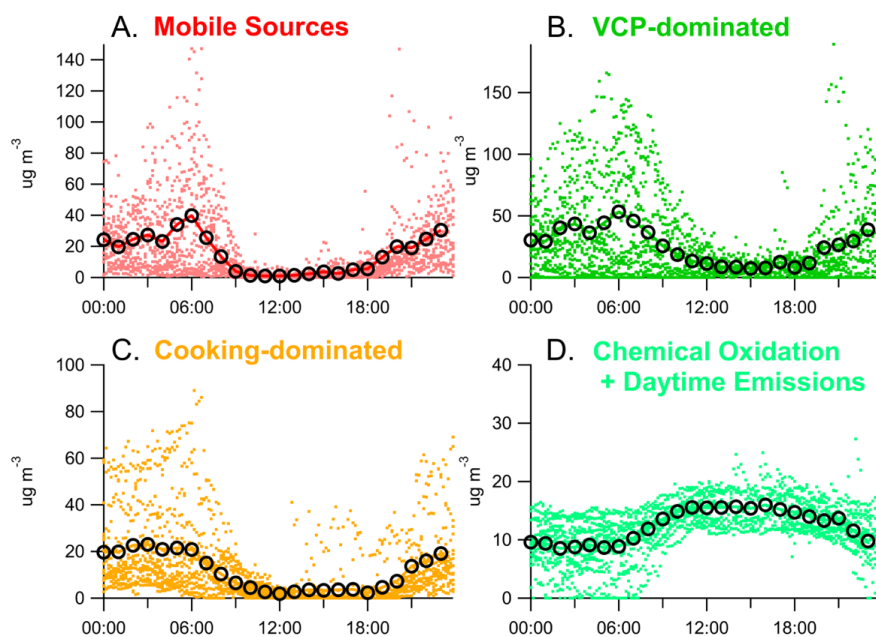
498
Figure 9: Diurnal patterns for the four factors resolved by PMF at the Jerome Mack ground site. The black
500   circles show the hourly mean values calculated over the full PMF solution.
501

502   To normalize for the impact of meteorology, Figure 10A shows the fraction that each primary
503   factor contributes total VOC mass resolved by PMF at the Jerome Mack ground site. Here, total
504   anthropogenic emissions are represented as the sum of the VCP-dominated, mobile source, and
505   cooking-dominated factors. The local solvent factor is excluded from this analysis since it is not
506   representative of regional VOC concentrations. Figure 10B shows the average PMF solution over
507   the entire analysis period.

508

509   Figure 10A shows that each factor contributes to the total anthropogenic emissions at different
510 times of day depending on the emission patterns. The VCP-dominated factor is the largest
511 contributor to total VOC emissions in Las Vegas and constitutes 40 – 80% of the primary VOCs
512 resolved by PMF. These concentrations are largely driven by the high emissions of solvents, such
513 as ethanol and acetone, which is consistent with observations from NYC (Gkatzelis et al., 2021b).
514 VCP emissions exhibit the highest relative abundances early in the day (~11:00 AM), then
515 decrease in relative abundance throughout the day. This behavior is similar to the diurnal pattern
516 of personal care product emissions observed in cities such as Boulder, CO where the mixing ratios
517 of D5-siloxane from deodorants and hair products peak during morning hours and decayed as
518 personal care products evaporate (Coggon et al., 2018). During evening and rush hour periods,
519 mobile sources constitute ~ 30-40% of the total primary VOC mixing ratios, but then decrease
520 during midday due to both a large enhancement of VCPs, but also lower emissions from mobile
521 sources. Over the entire dataset, VCPs and mobile sources are estimated to represent 54% and 25%
522 of the total anthropogenic VOCs, respectively (Fig. 10B).

523

524   The cooking-dominated factor represents 10-30% of the total primary VOC mass resolved by
525 PMF, depending on the time of day. The relative fraction of the cooking-dominated factor peaks
526 in the mid-afternoon, as well as in the evening and night when activity along the Las Vegas Strip
527 is highest. Similar behavior has been observed in the relative abundance of primary cooking
528 organic aerosol in cities such as Los Angeles (Hayes et al., 2013). The cooking-dominated factor
529 is estimated to represent as much as 21% of the total anthropogenic VOCs over the entire dataset.

530

531   The fraction of cooking VOCs estimated here (21%) is specific to a site downwind of the Las
532 Vegas Strip where restaurants are abundant. These impacts are likely to vary across urban areas
533 based on ground site locations, restaurant density, and differences in the proportions of fossil fuel
534 and VCP emissions. Cooking emissions are commonly resolved from the source apportionment of
535 organic aerosol measurements in US cities (e.g., Hayes et al., 2013;Lyu et al., 2019;Zhang et al.,
536 2019;Xu et al., 2015). Far fewer studies have estimated the impact of cooking on the outdoor VOC
537 burden in US urban areas. Recently, cooking emissions were identified from source apportionment
538 of thermal desorption aerosol gas chromatograms and shown to be present at significant mixing
539 ratios in Livermore, CA (Wernis et al., 2022). Similarly, source apportionment of PTR-ToF-MS
540 data from Atlanta, GA shows that cooking emissions mixed with biomass burning were
541 responsible for 6–15% of the reported VOC carbon, which included contributions from fossil fuel,
542 VCPs, and biogenic sources (Peng et al., 2022). These proportions are similar to those reported
543 here, suggesting that cooking VOCs represent a significant fraction of total anthropogenic VOCs
544 in other US cities. Table S1 summarizes the cooking profile resolved by the PMF analysis. This
545 profile could be used to compare against measurements of cooking VOCs in other urban areas.
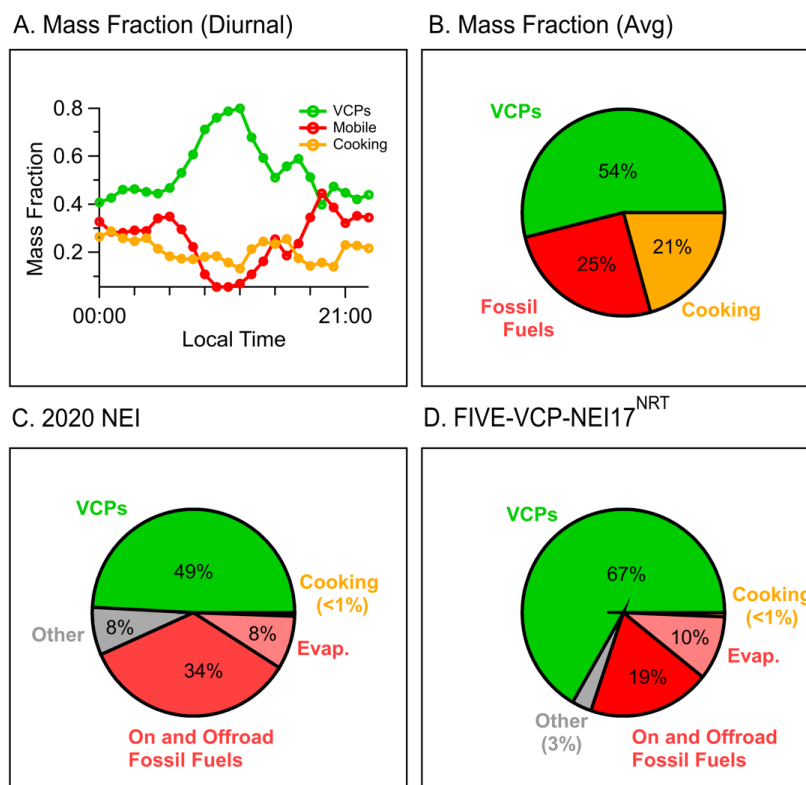
Figure 10: (A) Diurnal contribution of VCP, mobile sources, and cooking factors to the sum of primary emissions apportioned by PMF (= VCP + mobile source + cooking). (B) Average contribution of the VCP, mobile source, and mobile source factors to the PMF solution. (C) Distribution of anthropogenic VOC emissions from the 2020 National Emissions Inventory for Clark County, NV. (D) Distribution of anthropogenic VOCs from FIVE-VCP-NEI17^{NRT} in Clark County, NV. The "other" category in both inventories reflect emissions from industry, farming, and electric power generation.

5. Comparison to Inventory Emissions

The PMF results shown in Figure 10B are compared against the distribution of anthropogenic VOCs reported in emissions inventories used to model air quality (Figure 10, panels C and D). Panel C shows emissions reported in the 2020 National Emissions Inventory (NEI) for Clark County, NV. The NEI is a benchmark for determining US emissions standards and its methodology is fully described by the US Environmental Protection Agency (EPA, 2023). The NEI for Clark County includes emissions for mobile sources (e.g., on- and offroad vehicles), fossil fuel evaporative sources (e.g., gasoline stations), solvent evaporative sources (e.g., VCPs), and miscellaneous point and area sources. Cooking emissions in the NEI predominantly result from commercial sources with minor contributions from residential backyard barbequing.

19

566

567   Panel D shows the distribution of VOCs represented by the FIVE-VCP-NEI17[NRT] inventory
568   described by He et al. (2023). The FIVE-VCP inventory was developed following the methods
569   prescribed by McDonald et al. (2018) and was recently used to determine VCP impacts on air
570   quality in US cities (e.g., Coggon et al., 2021;Qin et al., 2021). He et al. (2023) updated FIVE-
571   VCP to include 2017 NEI emissions (NEI17) and revised VOC emissions with near real-time
572   (NRT) adjustment factors to account for COVID-19 impacts on various emission sectors. Mobile
573   source emissions are determined from fuel sales and on-road and off-road emission factors. VCP
574   emissions are estimated based on the mass balance of the chemical product industry for 2010 then
575   adjusted to 2021 emissions based on the long-term declining trends in VCP emissions reported by
576   Kim et al. (2022) and economic scaling factors reported by He et al. (2023). Other sectors are from
577   the NEI17 and are similarly updated with near real-time adjustment factors. Cooking emissions in
578   FIVE-VCP-NEI17[NRT] are the same as those used in the 2017 NEI.

579

580   The 2020 NEI and FIVE-VCP-NEI17[NRT] inventories both indicate that VCPs are the dominant
581   VOC emission sources in Clark County. Fossil fuel emissions are the next largest source, though
582   differences between the two inventories are evident. In the NEI, total fossil fuel emissions (= on-
583   and offroad emissions + evaporative emissions) are 15% lower than VCP emissions. In FIVE-
584   VCP-NEI17[NRT], fossil fuel emissions are 57% lower than VCPs. These differences are reflected
585   in previous comparisons between the NEI and FIVE-VCP (Coggon et al., 2021;McDonald et al.,
586   2018). The PMF solution shows that fossil fuels are ~54% lower than VCPs, which is most
587   consistent with FIVE-VCP-NEI17[NRT]. Zhu et al. (2023) show that FIVE-VCP speciation agrees
588   well with VOCs primarily emitted from fossil fuel and VCPs reported during SUNVEx and
589   RECAP-CA. Aldehydes, ethanol, and monoterpenes were underestimated which may point to the
590   importance of missing emission sources, such as cooking.

591

592   The fraction of total cooking VOC emissions represented in both inventories is significantly
593   lower than the fraction resolved by PMF. Commercial sources dominate the cooking emissions in
594   the 2017 and 2020 NEI and are estimated based on food consumption estimates and emission
595   factors derived from laboratory studies (e.g., Schauer et al., 1999). The differences between the
596   PMF results and what is reported in the inventories may be partially explained by the spatial scale
597   of the datasets – the inventories represent county-level emissions estimates, while the observations
598   are specific to a site strongly influenced by the Las Vegas Strip. Nevertheless, the magnitude of
599   the disconnect highlights the need for further analysis. It is possible that the emission factors and/or
600   consumption of oils, meats, and other foods are different from what is reflected in laboratory
601   studies.

602

603   **6. Conclusions**

604

605   Mobile laboratory and ground site measurements were analyzed to determine the importance
606   of cooking emissions on urban VOC composition in Las Vegas, NV. PTR-ToF-MS data show that
607   cooking is a significant source of long-chain aldehydes to urban air. Measurements of octanal and
608   nonanal are found to be useful markers to evaluate cooking emissions due to their abundance in
609   restaurant plumes and local enhancements in areas with high restaurant density. A comparison of
610   the mass spectra downwind of restaurants to those obtained in regions with significant commercial
611   cooking show similar distributions in aldehydes and fatty acids known to be emitted from
612   laboratory cooking experiments.

613

614   Based on a PMF analysis, it is estimated that cooking emissions represent as much as 20% of
615   the anthropogenic VOCs emitted to the atmosphere in Las Vegas, NV. It is expected that the
616   relative importance of cooking emissions in other cities will vary based on regional restaurant
617   density and the magnitude of other anthropogenic emissions including VCPs and mobile sources.
618   More work is needed to quantify cooking in other urban areas. Measurements from this study in
619   Pasadena, CA (Fig S12) and those conducted previously in Livermore, CA and Atlanta, GA show
620   that long-chain aldehydes are ubiquitous in urban air (~100 – 200 ppt) and modulated by
621   commercial and residential cooking (Wernis et al., 2022;Peng et al., 2022). The source
622   apportionment profiles determined here may be compared against other urban environments to
623   evaluate cooking in other cities.

624

625   The VOCs emitted from cooking are reactive and may contribute to the formation of ozone,
626   secondary organic aerosol, and other pollutants such as peroxyacyl nitrates (Bowman et al., 2003).
627   A review of VOC emissions inventories show that total cooking emissions (i.e., residential +
628   commercial cooking) are likely underrepresented in air quality models. Spatial patterns of long-
629   chain aldehydes suggest that more work is needed to quantify the magnitude of emissions from
630   commercial cooking, which are also important sources of primary urban SOA (Robinson et al.,
631   2018;Shah et al., 2018). PMF results in Las Vegas suggest that cooking emissions may be as
632   important to urban VOCs as mobile sources in regions with significant restaurant activity.

633

634   **Data Availability**

635

636   Data for SUNVEx and RE-CAP are available at the NOAA CSL data repository
637   (https://csl.noaa.gov/projects/sunvex/).

638

639   **Author Contribution**

640

641   MMC, CES, XL, JBG, AL, JP, HJB, KA, and CW conducted measurements during SUNVEx and
642   RE-CAP. CH, QZ, RHS, JH, ML, KS, and BC developed inventories used to compare against
643   observations. MMC and CW wrote the paper with contributions from all authors.

644

645   **Competing Interests**

646

661   **References**
662

663   Arata, C., Misztal, P. K., Tian, Y., Lunderberg, D. M., Kristensen, K., Novoselac, A., Vance, M. E.,
664   Farmer, D. K., Nazaroff, W. W., and Goldstein, A. H.: Volatile organic compound emissions
665   during HOMEChem, Indoor Air, 31, 2099-2117, https://doi.org/10.1111/ina.12906, 2021.

666   Bastos, L. C., and Pereira, P. A.: Influence of heating time and metal ions on the amount of free
667   fatty acids and formation rates of selected carbonyl compounds during the thermal oxidation of
668   canola oil, J Agric Food Chem, 58, 12777-12783, 10.1021/jf1028575, 2010.

669   Bowman, J. H., Barket, D. J., and Shepson, P. B.: Atmospheric Chemistry of Nonanal,
670   Environmental Science & Technology, 37, 2218-2225, 10.1021/es026220p, 2003.

671   Canonaco, F., Crippa, M., Slowik, J. G., Baltensperger, U., and Prévôt, A. S. H.: SoFi, an IGOR-
672   based interface for the efficient use of the generalized multilinear engine (ME-2) for the source
673   apportionment: ME-2 application to aerosol mass spectrometer data, Atmos. Meas. Tech., 6,
674   3649-3661, 10.5194/amt-6-3649-2013, 2013.

675   Churkina, G., Kuik, F., Bonn, B., Lauer, A., Grote, R., Tomiak, K., and Butler, T. M.: Effect of VOC
676   Emissions from Vegetation on Air Quality in Berlin during a Heatwave, Environmental Science &
677   Technology, 51, 6120-6130, 10.1021/acs.est.6b06514, 2017.

678   Coggon, M. M., Veres, P. R., Yuan, B., Koss, A., Warneke, C., Gilman, J. B., Lerner, B. M., Peischl,
679   J., Aikin, K. C., Stockwell, C. E., Hatch, L. E., Ryerson, T. B., Roberts, J. M., Yokelson, R. J., and de
680   Gouw, J. A.: Emissions of nitrogen-containing organic compounds from the burning of
681   herbaceous and arboraceous biomass: Fuel composition dependence and the variability of
682   commonly used nitrile tracers, Geophys. Res. Lett., 43, 9903-9912, 10.1002/2016gl070562,
683   2016.

684   Coggon, M. M., McDonald, B. C., Vlasenko, A., Veres, P. R., Bernard, F., Koss, A. R., Yuan, B.,
685   Gilman, J. B., Peischl, J., Aikin, K. C., DuRant, J., Warneke, C., Li, S. M., and de Gouw, J. A.:
686   Diurnal Variability and Emission Pattern of Decamethylcyclopentasiloxane (D5) from the
687   Application of Personal Care Products in Two North American Cities, Environ. Sci. Technol., 52,
688   5610-5618, 10.1021/acs.est.8b00506, 2018.

689   Coggon, M. M., Gkatzelis, G. I., McDonald, B. C., Gilman, J. B., Schwantes, R. H., Abuhassan, N.,
690   Aikin, K. C., Arend, M. F., Berkoff, T. A., Brown, S. S., Campos, T. L., Dickerson, R. R., Gronoff, G.,
691   Hurley, J. F., Isaacman-VanWertz, G., Koss, A. R., Li, M., McKeen, S. A., Moshary, F., Peischl, J.,
692   Pospisilova, V., Ren, X., Wilson, A., Wu, Y., Trainer, M., and Warneke, C.: Volatile chemical
693   product emissions enhance ozone and modulate urban chemistry, Proceedings of the National
694   Academy of Sciences, 118, e2026653118, doi:10.1073/pnas.2026653118, 2021.

695   Coggon, M. M., Stockwell, C. E., Claflin, M. S., Pfannerstill, E. Y., Lu, X., Gilman, J. B.,
696   Marcantonio, J., Cao, C., Bates, K., Gkatzelis, G. I., Lamplugh, A., Katz, E. F., Arata, C., Apel, E. C.,
697   Hornbrook, R. S., Piel, F., Majluf, F., Blake, D. R., Wisthaler, A., Canagaratna, M., Lerner, B. M.,
698   Goldstein, A. H., Mak, J. E., and Warneke, C.: Identifying and correcting interferences to PTR-
699   ToF-MS measurements of isoprene and other urban volatile organic compounds, EGUsphere,
700   2023, 1-41, 10.5194/egusphere-2023-1497, 2023.

701   de Gouw, J. A., Gilman, J. B., Kim, S.-W., Alvarez, S. L., Dusanter, S., Graus, M., Griffith, S. M.,
702   Isaacman-VanWertz, G., Kuster, W. C., Lefer, B. L., Lerner, B. M., McDonald, B. C., Rappenglück,
703   B., Roberts, J. M., Stevens, P. S., Stutz, J., Thalman, R., Veres, P. R., Volkamer, R., Warneke, C.,
704   Washenfelder, R. A., and Young, C. J.: Chemistry of Volatile Organic Compounds in the Los
705   Angeles Basin: Formation of Oxygenated Compounds and Determination of Emission Ratios,
706   Journal of Geophysical Research: Atmospheres, 123, 2298-2319,
707   https://doi.org/10.1002/2017JD027976, 2018.

708   US Environmental Protection Agency: 2020 National Emissions Inventory (NEI):
709   https://www.epa.gov/air-emissions-inventories/2020-national-emissions-inventory-nei-data,
710   2023.

711   Gentner, D. R., Worton, D. R., Isaacman, G., Davis, L. C., Dallmann, T. R., Wood, E. C., Herndon,
712   S. C., Goldstein, A. H., and Harley, R. A.: Chemical composition of gas-phase organic carbon
713   emissions from motor vehicles and implications for ozone production, Environ. Sci. Technol., 47,
714   11837-11848, 10.1021/es401470e, 2013.

715   Gkatzelis, G. I., Coggon, M. M., McDonald, B. C., Peischl, J., Aikin, K. C., Gilman, J. B., Trainer, M.,
716   and Warneke, C.: Identifying Volatile Chemical Product Tracer Compounds in U.S. Cities,
717   Environmental Science & Technology, 55, 188-199, 10.1021/acs.est.0c05467, 2021a.

718   Gkatzelis, G. I., Coggon, M. M., McDonald, B. C., Peischl, J., Gilman, J. B., Aikin, K. C., Robinson,
719   M. A., Canonaco, F., Prevot, A. S. H., Trainer, M., and Warneke, C.: Observations Confirm that
720   Volatile Chemical Products Are a Major Source of Petrochemical Emissions in U.S. Cities,
721   Environmental Science & Technology, 55, 4332-4343, 10.1021/acs.est.0c05471, 2021b.

722 Hayes, P. L., Ortega, A. M., Cubison, M. J., Froyd, K. D., Zhao, Y., Cliff, S. S., Hu, W. W., Toohey,
723 D. W., Flynn, J. H., Lefer, B. L., Grossberg, N., Alvarez, S., Rappenglück, B., Taylor, J. W., Allan, J.
724 D., Holloway, J. S., Gilman, J. B., Kuster, W. C., de Gouw, J. A., Massoli, P., Zhang, X., Liu, J.,
725 Weber, R. J., Corrigan, A. L., Russell, L. M., Isaacman, G., Worton, D. R., Kreisberg, N. M.,
726 Goldstein, A. H., Thalman, R., Waxman, E. M., Volkamer, R., Lin, Y. H., Surratt, J. D., Kleindienst,
727 T. E., Offenberg, J. H., Dusanter, S., Griffith, S., Stevens, P. S., Brioude, J., Angevine, W. M., and
728 Jimenez, J. L.: Organic aerosol composition and sources in Pasadena, California, during the 2010
729 CalNex campaign, Journal of Geophysical Research: Atmospheres, 118, 9233-9257,
730 10.1002/jgrd.50530, 2013.

731 He, J., Harkins, C., O'Dell, K., Li, M., Francoeur, C., Anenberg, S., Brown, S. S., Coggon, M. M.,
732 Frost, G. J., Gilman, J. B., Kongdragunta, S., Lamplugh, A., Pierce, B., Schwantes, R. H., Stockwell,
733 C. E., Warneke, C., Yang, K., and McDonald, B. C.: COVID-19 perturbation on US air quality and
734 human health impact assessment, in review., 2023.

735 Hurley, J. F., Smiley, E., and Isaacman-VanWertz, G.: Modeled Emission of Hydroxyl and Ozone
736 Reactivity from Evaporation of Fragrance Mixtures, Environmental Science & Technology, 55,
737 15672-15679, 10.1021/acs.est.1c04004, 2021.

738 Karl, T., Striednig, M., Graus, M., Hammerle, A., and Wohlfahrt, G.: Urban flux measurements
739 reveal a large pool of oxygenated volatile organic compound emissions, Proc. Natl. Acad. Sci.
740 U.S.A., 115, 1186-1191, 10.1073/pnas.1714715115, 2018.

741 Kilgour, D., Novak, G., and Bertram, T.: Observations of Biotic and Abiotic Marine Volatile
742 Organic Compounds Emitted from Coastal Seawater, December 01, 2021, 2021.

743 Kim, S.-W., McDonald, B. C., Seo, S., Kim, K.-M., and Trainer, M.: Understanding the Paths of
744 Surface Ozone Abatement in the Los Angeles Basin, Journal of Geophysical Research:
745 Atmospheres, 127, e2021JD035606, https://doi.org/10.1029/2021JD035606, 2022.

746 Klein, F., Farren, N. J., Bozzetti, C., Daellenbach, K. R., Kilic, D., Kumar, N. K., Pieber, S. M.,
747 Slowik, J. G., Tuthill, R. N., Hamilton, J. F., Baltensperger, U., Prevot, A. S., and El Haddad, I.:
748 Indoor terpene emissions from cooking with herbs and pepper and their secondary organic
749 aerosol production potential, Sci. Rep., 6, 36623, 10.1038/srep36623, 2016a.

750 Klein, F., Platt, S. M., Farren, N. J., Detournay, A., Bruns, E. A., Bozzetti, C., Daellenbach, K. R.,
751 Kilic, D., Kumar, N. K., Pieber, S. M., Slowik, J. G., Temime-Roussel, B., Marchand, N., Hamilton,
752 J. F., Baltensperger, U., Prévôt, A. S. H., and El Haddad, I.: Characterization of Gas-Phase
753 Organics Using Proton Transfer Reaction Time-of-Flight Mass Spectrometry: Cooking Emissions,
754 Environmental Science & Technology, 50, 1243-1250, 10.1021/acs.est.5b04618, 2016b.

755 Klein, F., Baltensperger, U., Prévôt, A. S. H., and El Haddad, I.: Quantification of the impact of
756 cooking processes on indoor concentrations of volatile organic species and primary and
757 secondary organic aerosols, Indoor Air, 29, 926-942, https://doi.org/10.1111/ina.12597, 2019.

758 Koss, A. R., Sekimoto, K., Gilman, J. B., Selimovic, V., Coggon, M. M., Zarzana, K. J., Yuan, B.,
759 Lerner, B. M., Brown, S. S., Jimenez, J. L., Krechmer, J., Roberts, J. M., Warneke, C., Yokelson, R.
760 J., and de Gouw, J.: Non-methane organic gas emissions from biomass burning: identification,
761 quantification, and emission factors from PTR-ToF during the FIREX 2016 laboratory
762 experiment, Atmos. Chem. Phys., 18, 3299-3319, 10.5194/acp-18-3299-2018, 2018.

763 Krechmer, J., Lopez-Hilfiker, F., Koss, A., Hutterli, M., Stoermer, C., Deming, B., Kimmel, J.,
764 Warneke, C., Holzinger, R., Jayne, J., Worsnop, D., Fuhrer, K., Gonin, M., and de Gouw, J.:
765 Evaluation of a New Reagent-Ion Source and Focusing Ion–Molecule Reactor for Use in Proton-
766 Transfer-Reaction Mass Spectrometry, Analytical Chemistry, 90, 12011-12018,
767 10.1021/acs.analchem.8b02641, 2018.

768 Kruza, M., Lewis, A. C., Morrison, G. C., and Carslaw, N.: Impact of surface ozone interactions on
769 indoor air chemistry: A modeling study, Indoor Air, 27, 1001-1011,
770 https://doi.org/10.1111/ina.12381, 2017.

771 Langford, A. O., Senff, C. J., Alvarez Ii, R. J., Aikin, K. C., Baidar, S., Bonin, T. A., Brewer, W. A.,
772 Brioude, J., Brown, S. S., Burley, J. D., Caputi, D. J., Conley, S. A., Cullis, P. D., Decker, Z. C. J.,
773 Evan, S., Kirgis, G., Lin, M., Pagowski, M., Peischl, J., Petropavlovskikh, I., Pierce, R. B., Ryerson,
774 T. B., Sandberg, S. P., Sterling, C. W., Weickmann, A. M., and Zhang, L.: The Fires, Asian, and
775 Stratospheric Transport–Las Vegas Ozone Study (FAST-LVOS), Atmos. Chem. Phys., 22, 1707-
776 1737, 10.5194/acp-22-1707-2022, 2022.

777 Liu, Y., Misztal, P. K., Arata, C., Weschler, C. J., Nazaroff, W. W., and Goldstein, A. H.: Observing
778 ozone chemistry in an occupied residence, Proceedings of the National Academy of Sciences,
779 118, e2018140118, doi:10.1073/pnas.2018140118, 2021.

780 Lyu, R., Alam, M. S., Stark, C., Xu, R., Shi, Z., Feng, Y., and Harrison, R. M.: Aliphatic carbonyl
781 compounds (C8–C26) in wintertime atmospheric aerosol in London, UK, Atmos. Chem. Phys.,
782 19, 2233-2246, 10.5194/acp-19-2233-2019, 2019.

783 McDonald, B. C., de Gouw, J. A., Gilman, J. B., Jathar, S. H., Akherati, A., Cappa, C. D., Jimenez, J.
784 L., Lee-Taylor, J., Hayes, P. L., McKeen, S. A., Cui, Y. Y., Kim, S. W., Gentner, D. R., Isaacman-
785 VanWertz, G., Goldstein, A. H., Harley, R. A., Frost, G. J., Roberts, J. M., Ryerson, T. B., and
786 Trainer, M.: Volatile chemical products emerging as largest petrochemical source of urban
787 organic emissions, Science, 359, 760-764, 10.1126/science.aaq0524, 2018.

788 McDonald, J. D., Zielinska, B., Fujita, E. M., Sagebiel, J. C., Chow, J. C., and Watson, J. G.: Fine
789 Particle and Gaseous Emission Rates from Residential Wood Combustion, Environmental
790 Science & Technology, 34, 2080-2091, 10.1021/es9909632, 2000.

791 Peng, C. Y., Lan, C. H., Lin, P. C., and Kuo, Y. C.: Effects of cooking method, cooking oil, and food
792 type on aldehyde emissions in cooking oil fumes, J Hazard Mater, 324, 160-167,
793 10.1016/j.jhazmat.2016.10.045, 2017.

794   Peng, Y., Mouat, A. P., Hu, Y., Li, M., McDonald, B. C., and Kaiser, J.: Source appointment of
795   volatile organic compounds and evaluation of anthropogenic monoterpene emission estimates
796   in Atlanta, Georgia, Atmospheric Environment, 288, 119324,
797   https://doi.org/10.1016/j.atmosenv.2022.119324, 2022.

798   Pye, H. O. T., Place, B. K., Murphy, B. N., Seltzer, K. M., D'Ambro, E. L., Allen, C., Piletic, I. R.,
799   Farrell, S., Schwantes, R. H., Coggon, M. M., Saunders, E., Xu, L., Sarwar, G., Hutzell, W. T., Foley,
800   K. M., Pouliot, G., Bash, J., and Stockwell, W. R.: Linking gas, particulate, and toxic endpoints to
801   air emissions in the Community Regional Atmospheric Chemistry Multiphase Mechanism
802   (CRACMM), Atmos. Chem. Phys., 23, 5043-5099, 10.5194/acp-23-5043-2023, 2023.

803   Qin, M., Murphy, B. N., Isaacs, K. K., McDonald, B. C., Lu, Q., McKeen, S. A., Koval, L., Robinson,
804   A. L., Efstathiou, C., Allen, C., and Pye, H. O. T.: Criteria pollutant impacts of volatile chemical
805   products informed by near-field modelling, Nature Sustainability, 4, 129-137, 10.1038/s41893-
806   020-00614-1, 2021.

807   Roberts, J. M., Neuman, J. A., Brown, S. S., Veres, P. R., Coggon, M. M., Stockwell, C. E.,
808   Warneke, C., Peischl, J., and Robinson, M. A.: Furoyl peroxynitrate (fur-PAN), a product of VOC–
809   NOx photochemistry from biomass burning emissions: photochemical synthesis, calibration,
810   chemical characterization, and first atmospheric observations, Environmental Science:
811   Atmospheres, 2, 1087-1100, 10.1039/D2EA00068G, 2022.

812   Robinson, A. L., Subramanian, R., Donahue, N. M., Bernardo-Bricker, A., and Rogge, W. F.:
813   Source Apportionment of Molecular Markers and Organic Aerosol. 3. Food Cooking Emissions,
814   Environmental Science & Technology, 40, 7820-7827, 10.1021/es060781p, 2006.

815   Robinson, E. S., Gu, P., Ye, Q., Li, H. Z., Shah, R. U., Apte, J. S., Robinson, A. L., and Presto, A. A.:
816   Restaurant Impacts on Outdoor Air Quality: Elevated Organic Aerosol Mass from Restaurant
817   Cooking with Neighborhood-Scale Plume Extents, Environmental Science & Technology, 52,
818   9285-9294, 10.1021/acs.est.8b02654, 2018.

819   Ryerson, T. B., Andrews, A. E., Angevine, W. M., Bates, T. S., Brock, C. A., Cairns, B., Cohen, R. C.,
820   Cooper, O. R., de Gouw, J. A., Fehsenfeld, F. C., Ferrare, R. A., Fischer, M. L., Flagan, R. C.,
821   Goldstein, A. H., Hair, J. W., Hardesty, R. M., Hostetler, C. A., Jimenez, J. L., Langford, A. O.,
822   McCauley, E., McKeen, S. A., Molina, L. T., Nenes, A., Oltmans, S. J., Parrish, D. D., Pederson, J.
823   R., Pierce, R. B., Prather, K., Quinn, P. K., Seinfeld, J. H., Senff, C. J., Sorooshian, A., Stutz, J.,
824   Surratt, J. D., Trainer, M., Volkamer, R., Williams, E. J., and Wofsy, S. C.: The 2010 California
825   Research at the Nexus of Air Quality and Climate Change (CalNex) field study, Journal of
826   Geophysical Research: Atmospheres, 118, 5830-5866, https://doi.org/10.1002/jgrd.50331,
827   2013.

828   Schauer, J. J., Kleeman, M. J., Cass, G. R., and Simoneit, B. R. T.: Measurement of Emissions from
829   Air Pollution Sources. 1. C1 through C29 Organic Compounds from Meat Charbroiling,
830   Environmental Science & Technology, 33, 1566-1577, 10.1021/es980076j, 1999.

831 Sekimoto, K., Li, S.-M., Yuan, B., Koss, A., Coggon, M., Warneke, C., and de Gouw, J.: Calculation
832 of the sensitivity of proton-transfer-reaction mass spectrometry (PTR-MS) for organic trace
833 gases using molecular properties, International Journal of Mass Spectrometry, 421, 71-94,
834 https://doi.org/10.1016/j.ijms.2017.04.006, 2017.

835 Shah, R. U., Robinson, E. S., Gu, P., Robinson, A. L., Apte, J. S., and Presto, A. A.: High-spatial-
836 resolution mapping and source apportionment of aerosol composition in Oakland, California,
837 using mobile aerosol mass spectrometry, Atmos. Chem. Phys., 18, 16325-16344, 10.5194/acp-
838 18-16325-2018, 2018.

839 Slowik, J. G., Vlasenko, A., McGuire, M., Evans, G. J., and Abbatt, J. P. D.: Simultaneous factor
840 analysis of organic particle and gas mass spectra: AMS and PTR-MS measurements at an urban
841 site, Atmos. Chem. Phys., 10, 1969-1988, 10.5194/acp-10-1969-2010, 2010.

842 Restaurant Inspections from the Southern Nevada Health District (SNHD).
843 https://opendataportal-lasvegas.opendata.arcgis.com/datasets/restaurant-inspections-open-
844 data/explore, 2022.

845 Stark, H., Yatavelli, R. L. N., Thompson, S. L., Kimmel, J. R., Cubison, M. J., Chhabra, P. S.,
846 Canagaratna, M. R., Jayne, J. T., Worsnop, D. R., and Jimenez, J. L.: Methods to extract
847 molecular and bulk chemical information from series of complex mass spectra with limited
848 mass resolution, International Journal of Mass Spectrometry, 389, 26-38,
849 https://doi.org/10.1016/j.ijms.2015.08.011, 2015.

850 Steinemann, A.: Volatile emissions from common consumer products, Air Qual. Atmos. Hlth., 8,
851 273-281, 10.1007/s11869-015-0327-6, 2015.

852 Steinemann, A. C., MacGregor, I. C., Gordon, S. M., Gallagher, L. G., Davis, A. L., Ribeiro, D. S.,
853 and Wallace, L. A.: Fragranced consumer products: Chemicals emitted, ingredients unlisted,
854 Environ. Impact. Asses., 31, 328-333, 10.1016/j.eiar.2010.08.002, 2011.

855 Stockwell, C. E., Coggon, M. M., Gkatzelis, G. I., Ortega, J., McDonald, B. C., Peischl, J., Aikin, K.,
856 Gilman, J. B., Trainer, M., and Warneke, C.: Volatile organic compound emissions from solvent-
857 and water-borne coatings – compositional differences and tracer compound identifications,
858 Atmos. Chem. Phys., 21, 6005-6022, 10.5194/acp-21-6005-2021, 2021.

859 Umano, K., and Shibamoto, T.: Analysis of acrolein from heated cooking oils and beef fat,
860 Journal of Agricultural and Food Chemistry, 35, 909-912, 10.1021/jf00078a014, 1987.

861 Wang, N., Ernle, L., Bekö, G., Wargocki, P., and Williams, J.: Emission Rates of Volatile Organic
862 Compounds from Humans, Environmental Science & Technology, 56, 4838-4848,
863 10.1021/acs.est.1c08764, 2022.

864 Warneke, C., de Gouw, J. A., Holloway, J. S., Peischl, J., Ryerson, T. B., Atlas, E., Blake, D.,
865 Trainer, M., and Parrish, D. D.: Multiyear trends in volatile organic compounds in Los Angeles,

866   California: Five decades of decreasing emissions, J. Geophs. Res., 117, 1-10,
867   10.1029/2012jd017899, 2012.

868   Wernis, R. A., Kreisberg, N. M., Weber, R. J., Drozd, G. T., and Goldstein, A. H.: Source
869   apportionment of VOCs, IVOCs and SVOCs by positive matrix factorization in suburban
870   Livermore, California, Atmos. Chem. Phys., 22, 14987-15019, 10.5194/acp-22-14987-2022,
871   2022.

872   Xu, L., Suresh, S., Guo, H., Weber, R. J., and Ng, N. L.: Aerosol characterization over the
873   southeastern United States using high-resolution aerosol mass spectrometry: spatial and
874   seasonal variation of aerosol composition and sources with a focus on organic nitrates, Atmos.
875   Chem. Phys., 15, 7307-7336, 10.5194/acp-15-7307-2015, 2015.

876   Yeoman, A. M., Shaw, M., Carslaw, N., Murrells, T., Passant, N., and Lewis, A. C.: Simplified
877   speciation and atmospheric volatile organic compound emission rates from non-aerosol
878   personal care products, Indoor Air, 30, 459-472, https://doi.org/10.1111/ina.12652, 2020.

879   Yuan, B., Koss, A., Warneke, C., Gilman, J. B., Lerner, B. M., Stark, H., and de Gouw, J. A.: A high-
880   resolution time-of-flight chemical ionization mass spectrometer utilizing hydronium ions (H3O+
881   ToF-CIMS) for measurements of volatile organic compounds in the atmosphere, Atmos. Meas.
882   Tech., 9, 2735-2752, 10.5194/amt-9-2735-2016, 2016.

883   Zhang, R., Lei, W., Tie, X., and Hess, P.: Industrial emissions cause extreme urban ozone diurnal
884   variability, Proceedings of the National Academy of Sciences, 101, 6346-6350,
885   doi:10.1073/pnas.0401484101, 2004.

886   Zhang, Y., Favez, O., Petit, J. E., Canonaco, F., Truong, F., Bonnaire, N., Crenn, V., Amodeo, T.,
887   Prévôt, A. S. H., Sciare, J., Gros, V., and Albinet, A.: Six-year source apportionment of submicron
888   organic aerosols from near-continuous highly time-resolved measurements at SIRTA (Paris area,
889   France), Atmos. Chem. Phys., 19, 14755-14776, 10.5194/acp-19-14755-2019, 2019.

890   Zhao, Y., and Zhao, B.: Emissions of air pollutants from Chinese cooking: A literature review,
891   Building Simulation, 11, 10.1007/s12273-018-0456-6, 2018.

892   Zhu, Q., Schwantes, R. H., Coggon, M. M., Harkins, C., Schnell, J., He, J., Pye, H. O. T., Li, M.,
893   Baker, B., Moon, Z., Ahmadov, R., Pfannerstill, E. Y., Place, B. K., Wooldridge, P., Schulze, B. C.,
894   Arata, C., Bucholtz, A., Seinfeld, J. H., Warneke, C., Stockwell, C. E., Xu, L., Zuraski, K., Robinson,
895   M. A., Neuman, J. A., Veres, P. R., Peischl, J., Brown, S. S., Goldstein, A. H., Cohen, R. C., and
896   McDonald, B. C.: A better representation of VOC chemistry and ozone over Los Angeles using
897   WRF-Chem, In prepration, 2023.
898